Downloaded from orbit.dtu.dk on: May 05, 2023

DTU Library

Longitudinal dispersion coefficients for numerical modeling of groundwater solute transport in heterogeneous formations

Lee, Jonghyun; Rolle, Massimo; Kitanidis, Peter K.

Published in:
Journal of Contaminant Hydrology

Link to article, DOI:
10.1016/j.jconhyd.2017.09.004

Publication date:
2018

Document Version
Peer reviewed version

Link back to DTU Orbit

Citation (APA):
Lee, J., Rolle, M., & Kitanidis, P. K. (2018). Longitudinal dispersion coefficients for numerical modeling of groundwater solute transport in heterogeneous formations. *Journal of Contaminant Hydrology*, *212*, 41-54. https://doi.org/10.1016/j.jconhyd.2017.09.004

General rights
Copyright and moral rights for the publications made accessible in the public portal are retained by the authors and/or other copyright owners and it is a condition of accessing publications that users recognise and abide by the legal requirements associated with these rights.

- Users may download and print one copy of any publication from the public portal for the purpose of private study or research.
- You may not further distribute the material or use it for any profit-making activity or commercial gain
- You may freely distribute the URL identifying the publication in the public portal

If you believe that this document breaches copyright please contact us providing details, and we will remove access to the work immediately and investigate your claim.

Accepted Manuscript

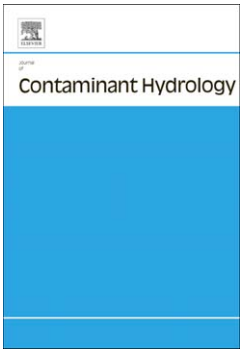

Longitudinal dispersion coefficients for numerical modeling of groundwater solute transport in heterogeneous formations

Jonghyun Lee, Massimo Rolle, Peter K. Kitanidis

PII: S0169-7722(17)30076-1
DOI: doi:10.1016/j.jconhyd.2017.09.004
Reference: CONHYD 3335

To appear in: *Journal of Contaminant Hydrology*

Received date: 20 March 2017
Revised date: 20 August 2017
Accepted date: 12 September 2017

Please cite this article as: Lee, Jonghyun, Rolle, Massimo, Kitanidis, Peter K., Longitudinal dispersion coefficients for numerical modeling of groundwater solute transport in heterogeneous formations, *Journal of Contaminant Hydrology* (2017), doi:10.1016/j.jconhyd.2017.09.004

This is a PDF file of an unedited manuscript that has been accepted for publication. As a service to our customers we are providing this early version of the manuscript. The manuscript will undergo copyediting, typesetting, and review of the resulting proof before it is published in its final form. Please note that during the production process errors may be discovered which could affect the content, and all legal disclaimers that apply to the journal pertain.

Longitudinal dispersion coefficients for numerical modeling of groundwater solute transport in heterogeneous formations

Jonghyun Lee[1,2,*], Massimo Rolle[3], Peter K. Kitanidis[1]

Abstract

Most recent research on hydrodynamic dispersion in porous media has focused on whole-domain dispersion while other research is largely on laboratory-scale dispersion. This work focuses on the contribution of a single block in a numerical model to dispersion. Variability of fluid velocity and concentration within a block is not resolved and the combined spreading effect is approximated using resolved quantities and macroscopic parameters. This applies whether the formation is modeled as homogeneous or discretized into homogeneous blocks but the emphasis here being on the latter. The process of dispersion is typically described through the Fickian model, *i.e.*, the dispersive flux is proportional to the gradient of the resolved concentration, commonly with the Scheidegger parameterization, which is a particular way to compute the dispersion coefficients utilizing dispersivity coefficients. Although such parameterization is by far the most commonly used in solute transport applications, its validity has been questioned. Here, our goal is to investigate the effects of heterogeneity and mass transfer limitations on block-scale longitudinal dispersion and to evaluate under which conditions the Scheidegger parameterization is valid. We compute the relaxation time

*Corresponding author

Email addresses: jonghyun.harry.lee@hawaii.edu (Jonghyun Lee), masro@env.dtu.dk (Massimo Rolle), peterk@stanford.edu (Peter K. Kitanidis)

[1]Department of Civil and Environmental Engineering, Stanford University, 473 Via Ortega, Stanford, CA, 94305, USA

[2]Department of Civil and Environmental Engineering and Water Resources Research Center, University of Hawaii at Manoa, Honolulu, HI, 96822, USA

[3]Department of Environmental Engineering,Technical University of Denmark, 2800 Kgs., Lyngby, Denmark

or memory of the system; changes in time with periods larger than the relaxation time are gradually leading to a condition of local equilibrium under which dispersion is Fickian. The method we use requires the solution of a steady-state advection-dispersion equation, and thus is computationally efficient, and applicable to *any* heterogeneous hydraulic conductivity K field without requiring statistical or structural assumptions. The method was validated by comparing with other approaches such as the moment analysis and the first order perturbation method. We investigate the impact of heterogeneity, both in degree and structure, on the longitudinal dispersion coefficient and then discuss the role of local dispersion and mass transfer limitations, *i.e.*, the exchange of mass between the permeable matrix and the low permeability inclusions. We illustrate the physical meaning of the method and we show how the block longitudinal dispersivity approaches, under certain conditions, the Scheidegger limit at large Péclet numbers. Lastly, we discuss the potential and limitations of the method to accurately describe dispersion in solute transport applications in heterogeneous aquifers.

Keywords: Longitudinal dispersion, numerical models, solute transport, heterogeneity and scale

---

1. Introduction

Accurate prediction of solute transport spreading and mixing is crucial for safe and reliable subsurface management applications. The fundamental processes that control flow and solute transport in geologic formations have been studied extensively both in the laboratory and through mathematical analysis. For example, in the transport of a conservative solute subject to advection and molecular diffusion, at the pore scale the solute concentration satisfies an advection-diffusion equation. The velocity satisfies the Stokes (*i.e.*, low Reynolds number hydrodynamics) equation and diffusion follows Fick's law. The number of pore-scale studies of solute transport has dramatically increased in recent years and these investigations have certainly contributed to improve our understanding of solute transport in porous media [e.g. 1, 2, 3, 4, 5, 6]. However, in Hydrogeologic applications, solute transport is still a formidable challenge because modeling is done at much larger scales.

Since geologic media exhibit heterogeneity at multiple scales, the variability of physical and chemical properties results in complex transport be-

haviors [7]. In current practice, flow and transport simulations are generally performed for a homogeneous medium, the approach preferred in analytical methods, or what effectively is spatially distributed homogeneous blocks, the approach followed in finite-element and finite-volume methods. The process of representing quantitatively the effect of unresolved variability in terms of resolved quantities is the problem of *parameterization*. For the flow problem, Darcy's law is used, meaning the velocity is proportional to hydraulic head gradient, and its validity is seldom disputed. For solute transport, the effect of unresolved velocity in combination with unresolved concentration is much more difficult to capture [8, 9, 10, 11, 12]. However, this effect is quite pronounced when dealing with plumes hundreds of meters long and with grid spacing of the order of meters or more.

In practice, the most widely used dispersion modeling approach is the Fickian model with Scheidegger parameterization [13], where dispersion coefficients are computed from constant dispersivity coefficients, considered medium properties and independent of molecular diffusion and flow velocity. The Scheidegger parameterization was originally justified based on a random-walk model dominated by advection in macroscopically homogeneous media. This approach has been the subject of intense scrutiny.

2. Overview of Objectives and Approach

Much work has been done on dispersion in the last thirty years, which makes it imperative to explain our perspective and our approach before we embark on the analysis or show any results. Consider a geologic formation that is heterogeneous at all scales. This is modeled using a numerical model that subdivides the domain under study on the basis of a numerical grid. To fix ideas, consider that we divide the domain into blocks, each of which is modeled as a continuum with appropriate properties. For example, a block consisting of potentially different sedimentary facies is modeled as a uniform block subject to Darcy's law with certain conductivity parameters. In principle, there is a fine-scale description, represented by a velocity that varies at the scale of micrometers, and a coarse-scale description represented by a specific discharge that varies at the scale of the grid, which may be of the order of meters. The objective is that the two descriptions should yield the same results at the scale of variability captured by the grid. In other words, whether one resolves the fine-scale variability and solves the Navier-Stokes and advection-diffusion equations or one solves the much simpler groundwa-

ter flow and transport problems with a homogeneous block, one would obtain the same results after averaging the fine-scale result to the scale of the grid.

What we just described is the basic idea underlying the continuum approach. This approach works well in making the transition from the molecular scale to the fluid-mechanical scale, where for example the fine scale may represent a very large number of interacting water molecules shifting position and the macroscopic scale is a uniform fluid with given density and viscosity. In Hydrogeology we are faced with a similar problem but we must deal with heterogeneity at many scales, from the scale of a pore to that of a formation. The practical solution already mentioned is to resolve larger-scale variability through a grid and apply the continuum approach to each block. But there are persistent challenges. Is there a manageable coarse-scale model, under what conditions is this model appropriate, and what error is to be expected from its application?

The problem we will address is that of dispersion of conservative nonreactive solutes and how to parameterize it in the context of a numerical model. The majority of papers on dispersion have examined the problem of whole-domain dispersion in formations with some regularity, such as random media [14, 15, 16], as it would apply in the transport of a large plume. Only a few works [17, 18, 19, 20, 21, 22] have studied the problem of what dispersion coefficients to assign to blocks in a numerical model and notable examples that have dealt with such problem include the approach developed by Rubin et al. [18], as well as the recent work by de Barros and Dentz [22]. The problem of block-scale dispersion is also the main focus of this study, which has the specific objectives of (i) explaining and visualizing how block-scale longitudinal dispersion originates from the velocity and concentration fluctuations within the block, (ii) investigating the interplay between advection and diffusive mass transfer rate for a range of flow velocities and permeability contrasts common in hydrogeologic applications, (iii) analyzing under what conditions the common Scheidegger method of describing dispersion is valid, and (iv) perform error quantification for this parameterization.

While previous studies have made assumptions regarding the structure, such as periodic or stationary, we present a method of analysis that does not require a specific structure for the formation as a whole or even for the individual block. And while much of recently published work deals with non-equilibrium conditions and non-Fickian transport [23, 24], this work focuses on the Fickian model. When we say Fickian, we mean at the scale of a block and we do not imply macroscopically homogeneous media, like stationary

conductivity, or Gaussian shaped plumes. One can actually model irregular plumes by resolving heterogeneity at the scale of a grid chosen for the needs of a particular application. The proposed approach is in the spirit of the times, which is to recognize the importance of heterogeneity and the ability to better resolve heterogeneity thanks to technological trends like faster computations, better sensing technologies, and the ability to invert data to estimate parameters [e.g., 25, 26, 27]. We will argue that as we can deal with increasingly finer grid, the Fickian model becomes a more accurate representation of transport because the key requirement, that of local equilibrium, is better met. Local equilibrium implies conditions sufficiently independent from an external perturbation, with gradual changes and a dynamic balance between velocity variability causing concentration fluctuations and the opposing effect of diffusion.

There have been many computational studies on dispersion [e.g., 28, 29, 30]. The majority of them, particularly the most recent and most elaborate and comprehensive of them, have been performed in a Lagrangian framework and with purpose of describing the early and late behavior of dispersion in large statistically homogeneous formations. The Lagrangian perspective focuses on following particles or the statistics of particles as they move in time and space. Landmarks in the development of this approach to study dispersion include Taylor [31], Scheidegger [13], and Dagan [32]. It appears that most informed Hydrogeologists consider the Lagrangian perspective as the most natural and useful approach for conceptualization and analysis of dispersion. By contrast, this is a computational study based on a theory developed in an Eulerian framework, which focuses on computing the contribution of a block to dispersive transport. Important steps in the development of this approach were Bensoussan et al. [33] and Brenner [34], who considered transport in an idealized periodic medium and evaluated dispersion coefficients that are properties of the formation; however, all computations boil down to solving a boundary-value problem in one block. Because of their emphasis on an idealized case and their heavily mathematical treatment, these works did not attract much attention in the Hydrogeologic literature, with a few notable exceptions [35, 36, 37]. The approach of Gelhar and Axness [38], who focused on unbounded domains, stationary media, and analytic methods, is also related to the same general methodology.

In this study we adopt an Eulerian approach which is intuitively appealing and easy to explain, at least with respect to the basic ideas. Instead of following particles, which enter and exit the block of interest, we focus on the

velocity inside the block. The velocity consists of the mean plus fluctuations about the mean. The effect of the mean velocity is captured by advective transport. The fluctuations have zero mean but if there is a concentration gradient, these zero-mean velocity fluctuations will have a net effect: they will transport mass downgradient in what is known as dispersive transport. Furthermore, this transport is proportional to the concentration gradient, which is the essence of Fickian transport. This is the essence of the analysis we carry out in the next section.

The analysis is along lines similar to those of previous Eulerian theories but with some important differences. We focus on a single block and make no assumptions about structure of heterogeneity *outside of the block*. This means that there is an indeterminacy from unknown boundary conditions, or the interaction with surrounding blocks, that in previous studies was assumed to vanish under restrictive conditions about structure. Our approach is not to make such assumptions but instead to perform uncertainty quantification. We show that the effect is minor for large velocity cases for which dispersion is important.

One computational advantage of the Eulerian approach for the study of dispersion is that its application requires the solution of steady transport problems, unlike the Lagrangian approach. The results do not depend on initial concentration but the velocity field and the local diffusion-dispersion coefficients. However, the theory assumes that conditions approach a state of local equilibrium and in this paper we discuss what local equilibrium means and examine the question of how rapidly local equilibrium can be achieved.

3. Method

A method to compute dispersion coefficients for a heterogeneous block starting from three-dimensional pore-scale Stokes flow and advection diffusion has been presented in Kitanidis [39]. However, solving this problem in a block of the order of 1 m^3 would require a tremendous computational effort and exorbitant amounts of information on the geometry of pore space, for example existing works such as Bijeljic et al. [40] are limited to a block of the order of 1 cm^3, so direct numerical simulation is postponed for future investigation. Here, we will derive the same result starting from the continuum-scale models of Darcy flow and advection-dispersion with local coefficients.

Under the continuity condition $\nabla \cdot \boldsymbol{q} = 0$, the advection-dispersion equation that is commonly used to model transport in porous media is:

$$\frac{\partial(\theta C)}{\partial t} + \nabla \cdot (\boldsymbol{q}C - \theta \boldsymbol{D}_{\text{local}} \nabla C) = 0 \tag{1}$$

where C is the point concentration in the continnum scale [-], θ is the porosity [-], $\boldsymbol{q}$ is the Darcy velocity (i.e., specific discharge) $[L/T]$, and $\boldsymbol{D}_{\text{local}}$ is the local dispersion tensor $[L^2/T]$. Let Ω be the heterogeneous block for which we want to compute the effective value of hydrodynamic dispersion. To keep the analysis simple, we will consider that θ is constant over this block, focusing on variability of specific discharge caused by variability in hydraulic conductivity. Starting from Eq. 1, the objective is to show that, as assumed in numerical models, the equation of mass conservation over the block Ω is given by

$$\int_{\Omega} \left[\frac{\partial \bar{C}}{\partial t} + \nabla \cdot \left(\bar{\boldsymbol{u}} \bar{C} - \boldsymbol{D}_{\Omega} \nabla \bar{C} \right) \right] dV = 0 \tag{2}$$

where $\bar{C}$, $\bar{\boldsymbol{u}}$ and $\boldsymbol{D}_{\Omega}$ are the resolved (large-scale) concentration [-], linear velocity $[L/T]$, and "block-effective" dispersion tensor $[L^2/T]$, respectively. The finer the volume Ω is, the better the Fickian model in Eq. 2 predicts.

Using Reynolds decomposition [e.g. 41, 42, 43], the actual concentration $C(t, x, y, z)$ that satisfies the fine-scale transport equation (Eq. 1) can be modeled as consisting of two components:

$$C(t, x, y, z) = \bar{C}(t, x, y, z) + C'(t, x, y, z) \tag{3}$$

where $\bar{C}$ is the resolved concentration at the scale of Ω and C' is the fluctuation around $\bar{C}$, so that $\int_{\Omega} C' dV = 0$. The concentration C' represents the unresolved or subgrid variability. Under gradually varying conditions in space and time, $\bar{C}$ varies gradually at the scale of Ω while most of the variability of C' is at scales smaller than the scale of the support volume so that any average of related quantities to C' over Ω is negligible. Similarly we represent $\boldsymbol{u}$ as

$$\boldsymbol{u}(t, x, y, z) = \bar{\boldsymbol{u}}(t, x, y, z) + \boldsymbol{u'}(t, x, y, z) \tag{4}$$

where $\bar{\boldsymbol{u}}$ is the average velocity at the scale Ω and $\boldsymbol{u'}$ is the velocity fluctuation about $\bar{\boldsymbol{u}}$. As for the concentration fluctuation, also the volume average of $\boldsymbol{u'}$ is zero. By substituting Eqs. 3 and 4 into the fine-scale transport equation (Eq. 1) we obtain:

$$\frac{\partial \bar{C}}{\partial t}+\frac{\partial C'}{\partial t}+\nabla\cdot\left(\bar{\boldsymbol{u}}\bar{C}+\bar{\boldsymbol{u}}C'+\boldsymbol{u}'\bar{C}+\boldsymbol{u}'C'\right)-\nabla\cdot\left(\boldsymbol{D}_{\text{local}}\nabla\bar{C}+\boldsymbol{D}_{\text{local}}\nabla C'\right)=0 \tag{5}$$

Integrating Eq. 5 over the block Ω and considering that $\boldsymbol{u}'$ and C' are averaged out to be zero, $\int_\Omega \left[\frac{\partial C'}{\partial t}+\nabla\cdot\left(\bar{\boldsymbol{u}}C'+\boldsymbol{u}'\bar{C}\right)-\nabla\boldsymbol{D}_{\text{local}}\cdot\nabla C'\right]\theta dV$ can be neglected with a small loss of accuracy, we eventually have

$$\int_\Omega\left[\frac{\partial \bar{C}}{\partial t}+\nabla\cdot\left(\bar{\boldsymbol{u}}\bar{C}\right)+\nabla\cdot\left(\boldsymbol{u}'C'\right)-\nabla\cdot\left(\boldsymbol{D}_{\text{local}}\nabla\bar{C}\right)\right]dV=0 \tag{6}$$

We will focus on how to represent the nonzero term $\nabla\cdot(\boldsymbol{u}'C')$, which represents dispersive transport due to subgrid variability, in terms of resolved variability and constituent parameters.

Under the condition of gradual concentration changes, the resolved concentration $\bar{C}$ within the block can be approximated as [39]:

$$\bar{C}(t,x,y,z)=A+a_1(x-\bar{u}_1t)+a_2(y-\bar{u}_2t)+a_3(z-\bar{u}_3t) \tag{7}$$

where A, a_1, a_2, a_3 are constants. This simplification reflects that the concentration $\bar{C}$ is varying in space in the smoothest fashion, which is linear, and satisfies the grid-scale transport equation. The slopes of the macroscopic concentration $\nabla\bar{C}$ are then the coefficients a:

$$\nabla\bar{C}=\begin{bmatrix}\frac{\partial\bar{C}}{\partial x}\\ \frac{\partial\bar{C}}{\partial y}\\ \frac{\partial\bar{C}}{\partial z}\end{bmatrix}=\begin{bmatrix}a_1\\ a_2\\ a_3\end{bmatrix} \tag{8}$$

Considering the fine-scale mass conservation (Eq. 5) and substituting the approximate solution for $\bar{C}$ (Eq. 7), we find that C' satisfies

$$\frac{\partial C'}{\partial t}+\nabla\cdot(\boldsymbol{u}C')-\nabla\cdot(\boldsymbol{D}_{\text{local}}\nabla C')=-a_1u_1'-a_2u_2'-a_3u_3' \tag{9}$$

Since slow changes are assumed, we neglect $\frac{\partial C'}{\partial t}$ focusing on the quasi-steady condition. We will discuss this issue in the next section.

Because of the linearity of this equation, the superposition principle holds, meaning that the solution to Eq. 9 is given by

$$C'=-f_1a_1-f_2a_2-f_3a_3 \tag{10}$$

where each of the f terms satisfies

$$\nabla \cdot (\boldsymbol{u} f_i) - \nabla \cdot (\boldsymbol{D}_{\text{local}} \nabla f_i) = u_i' \quad \text{for } i = 1, 2 \text{ and } 3 \tag{11}$$

Note that if f_i satisfies this equation, so does $f_i + const.$, but the solution must have zero mean, since C' has zero spatial average. To finalize the solution, appropriate boundary conditions must be used and this issue will be discussed in the next section.

The dispersive flux term $\boldsymbol{u'}C'$ in Eq. 6 is now written as

$$\boldsymbol{u'}C' = -\begin{bmatrix} u_1' \\ u_2' \\ u_3' \end{bmatrix} (f_1 a_1 + f_2 a_2 + f_3 a_3) \tag{12}$$

$$= \begin{bmatrix} u_1' f_1 & u_1' f_2 & u_1' f_3 \\ u_2' f_1 & u_2' f_2 & u_2' f_3 \\ u_3' f_1 & u_3' f_2 & u_3' f_3 \end{bmatrix} \begin{bmatrix} a_1 \\ a_2 \\ a_3 \end{bmatrix} \tag{13}$$

As a result, the dispersion is Fickian, i.e., the dispersive flux is expressed as the product of second-order tensor and the concentration gradient (Eq. 8) (cf. [33, 34, 36, 37, 44]). Thus, Fickian behavior follows from the state of local equilibrium, which is the assumption we made in Eq. 7. Upscaled, effective dispersion coefficient over the block is given by

$$\int_\Omega \boldsymbol{u'}C' dV = \int_\Omega \boldsymbol{D}_\Omega \nabla \bar{C} dV \tag{14}$$

where the block-scale dispersion tensor $\boldsymbol{D}_\Omega$ is expressed as:

$$D_{\Omega,ij} = \frac{\int_\Omega u_i' f_j dV}{V_\Omega} \tag{15}$$

The approach allows one to quantitatively assess the role of 1) structure of heterogeneity, 2) degree of heterogeneity, and 3) advection and local diffusion-dispersion processes on block dispersion. Note that the proposed approach is applicable to any heterogeneous hydraulic conductivity field and only requires the steady-state equations in Eq. 11 instead of solving the entire ADE at the local scale. If more than a single dispersion coefficient for grid blocks of a large model are considered, the steady-state equations are simply repeated efficiently for each individual grid block, which can be accelerated further by using parallel programming and reusing preconditioner matrix. Though the

approach can be used to compute all components of the tensor, we will focus exclusively on the longitudinal dispersion coefficient D_L (the term also commonly denoted as D_{11} or D_{xx}), requiring the computed f_1 from the solution of Eq. 11.

4. Computational Experiments

Consider a block with intermixed regions of coarse and fine sand, similar to the systems investigated previously in flow-through laboratory experiments [8, 45, 11]. This is a quasi 2-D flow-through chamber with dimensions of 0.86 $m \times 0.45$ m in the x and z directions, respectively. Four different heterogeneity structures for conductivity K, shown in Figure 1, are considered to study the effect of spatial heterogeneity structure on the block-effective dispersion over the entire flow-through chamber. Each configuration (Figure 1 (a) - (d)) is filled with a homogeneous coarse sand with $K = 5 \times 10^{-3}$ m/s and several homogeneous low-K rectangular inclusions with different lengths, designed to occupy $\sim 16\%$ of the domain. While a sand with $K = 1.4 \times 10^{-4}$ m/s was used for the low-permeability inclusions in the original experiment, in the present work we computed results for four different K values: 1.4×10^{-3}, 1.4×10^{-4}, 1.4×10^{-5}, and 1.4×10^{-6} m/s for the low-permeability material to study the effect of the magnitude of heterogeneity. The porosity θ [-] of the medium is assumed to be 0.4.

Ideally, one should perform direct numerical simulation of pore-scale three-dimensional flow and transport. However, such a simulation would involve a tremendous number of grains for a block of this size. Instead, in this work an almost direct numerical simulation will be performed, in which microscopic processes are modeled at the continuum (*i.e.*, Darcy flow and ADE transport) with a fine grid of 0.001 m in both x and z. Local hydrodynamic dispersion coefficients were described according to parameterizations developed from detailed experimental investigation of dispersion in flow-through porous media [46, 47]:

$$D_{L,\text{local}} = D_p + \frac{1}{2} ud \tag{16}$$

$$D_{T,\text{local}} = D_p + \frac{ud}{\sqrt{Pe + 123}} \tag{17}$$

where D_p [m^2/s] is the pore diffusion coefficient (i.e., the aqueous diffusion coefficient D_{aq} corrected by the tortuosity of the porous medium), d [m] is

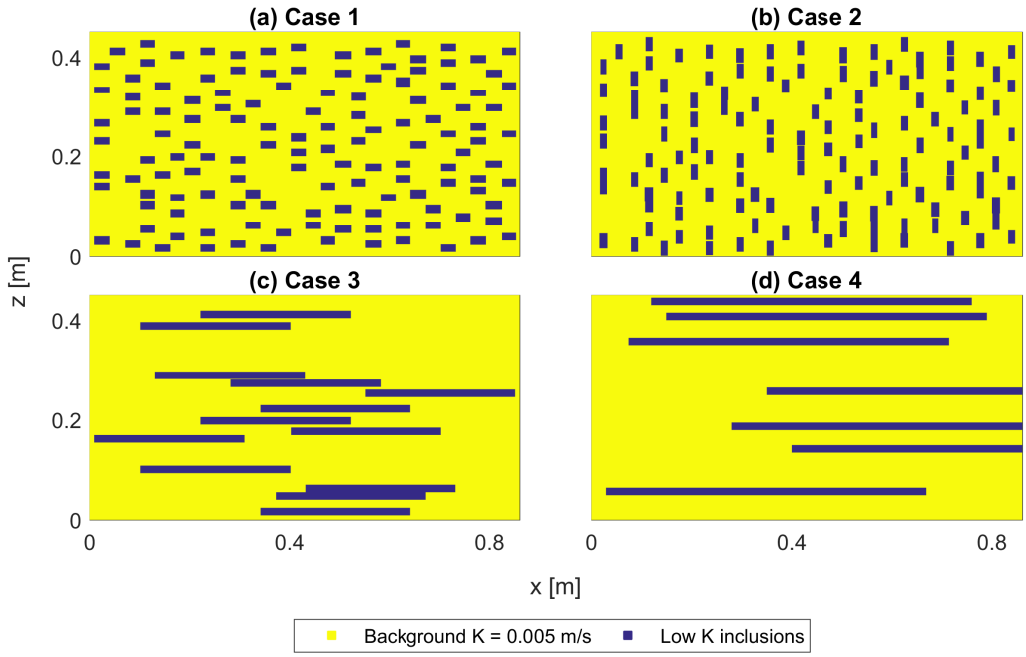

Figure 1: Hydraulic conductivity fields with (a) 135 low permeability inclusions (1.5×3 cm), (b) 135 low permeable inclusions (3×1.5 cm), (c) 13 low permeability inclusions (1.5×30 cm), (d) 7 low permeable inclusions (15×64 cm).

the grain size diameter that is consistent with the conductivity, u is the mean linear velocity, and $Pe = ud/D_{aq}$ [-] is the grain Péclet number. These parameterizations of local dispersion coefficients were selected because of their simplicity and capability to capture the longitudinal and lateral dispersion behavior observed in a large number of flow-through experiments in unconsolidated porous media. For instance, in longitudinal direction, linear (Eq. 16) or weakly nonlinear ($D_L \sim Pe^{1.1-1.2}$) equations for D_L have shown good agreement with solute breakthrough data obtained in a range of flow conditions relevant for groundwater flow [e.g., 46, 48, 49]. In the lateral direction, local D_T is important for the exchange of mass in heterogeneous media. The nonlinear, compound-specific description (Eq. 17) has been tested in a large number of experiments in quasi 2-D and fully 3-D setups using different tracers and porous media [e.g. 47, 50, 51, 52] and has been supported by pore-scale numerical simulations [53, 54]. An important feature of Eqs. 16 and 17 is that they allow a spatially variable representation of local hydrodynamic dispersion that can be directly linked to the spatially variable conductivity of heterogeneous porous media. Different empirical correlations have been proposed to relate the hydraulic conductivity to the grain size of unconsolidated materials; in this study we use the approximation of Hazen [55], which was adopted in previous simulations of solute transport in heterogeneous media [e.g., 56, 57], and suggests a simple square root relation:

$$d \approx c\sqrt{K} \tag{18}$$

where c is an empirical constant of proportionality $[L^{1/2}T^{1/2}]$. The exact value of c varies from study to study but we determined $c = 0.015$ from the actual sand properties used in Levy and Berkowitz [11] in order to find the grain sizes for various K values used in this study. Here K is in m/s and d is in m. Table 1 lists the values of the grain sizes for the permeable matrix and for the low-permeability inclusions with different hydraulic conductivity, considered in our computational experiments.

A mixed finite element method is implemented to obtain the local velocity u and a streamline-based transport simulator [58] is used to minimize numerical dispersion. The first step is to solve Eq. 11 subject to boundary conditions to compute f_1. The value of f_1 depends primarily on the velocity fluctuations u_1' inside the block and to a lesser extent on conditions in surrounding blocks, through the boundary conditions. For simplicity, we will consider as basic case for boundary conditions $f_1 = constant$. After the solution is obtained, the spatial average of the solution f_1 is subtracted from

	Hydraulic Conductivity (m/s)	Grain Diameter (m)
Background coarse sands	5×10^{-3}	1.1×10^{-3}
Inclusions	1.4×10^{-3}	5.6×10^{-4}
	1.4×10^{-4}	1.8×10^{-4}
	1.4×10^{-5}	5.6×10^{-5}
	1.4×10^{-6}	1.8×10^{-5}

Table 1: Properties of the porous media tested in the simulation.

the values of f_1 obtained by Eq. 11 and we will be using the zero-mean f_1' to plot results and compute the dispersion coefficient in equation (Eq. 15). The results are identical for any value of the *constant* we choose for the boundary condition. We will perform sensitivity analysis on the effect of different boundary conditions on the computed block-effective dispersion later.

For an initial confirmation that the results are reasonable, we compared the longitudinal dispersion coefficient determined from second central moment of a tracer plume using numerical simulations with the one computed from our method for Case 1 with low permeable inclusions of $K = 1.4 \times 10^{-4}\ m/s$ ($\mathrm{var}(\ln K) = 1.69$). Following an experiment setup of Levy and Berkowitz [11], spike dye injection at five locations (cf. Figure 8 in Levy and Berkowitz [11]) were simulated with a constant flow rate of 6.5 ml/min ($\bar{u} = 6 \times 10^{-6}$ m/s) as in Figure 2. Based on the relationship between the spatial moments of a plume and the transport parameters [59], the longitudinal dispersion coefficient for a medium with constant porosity is computed as

$$D_L = \frac{1}{2}\frac{dm_2(t)}{dt} \tag{19}$$

$$m_2(t) = \frac{\int_0^\infty \int_0^\infty (x-\mu(t))^2 C(x,y,t)dxdy}{\int_0^\infty \int_0^\infty C(x,y,t)dxdy} \tag{20}$$

$$\mu(t) = \frac{\int_0^\infty \int_0^\infty xC(x,y,t)dxdy}{\int_0^\infty \int_0^\infty C(x,y,t)dxdy} \tag{21}$$

where m_2 is the normalized second central moment in x direction and $C(x,t)$ is the concentration at the location x and time t. In Figure 3, we plot the second central spatial moment of the plumes and display the dispersion coefficient. D_L from two methods are $1.46 \times 10^{-7}\ m^2/s$ (from Eq. 15) and $1.60 \times 10^{-7}\ m^2/s$ (from Eq. 19), respectively. The relative difference of about 8% in these two values for the effective longitudinal dispersion coefficient is

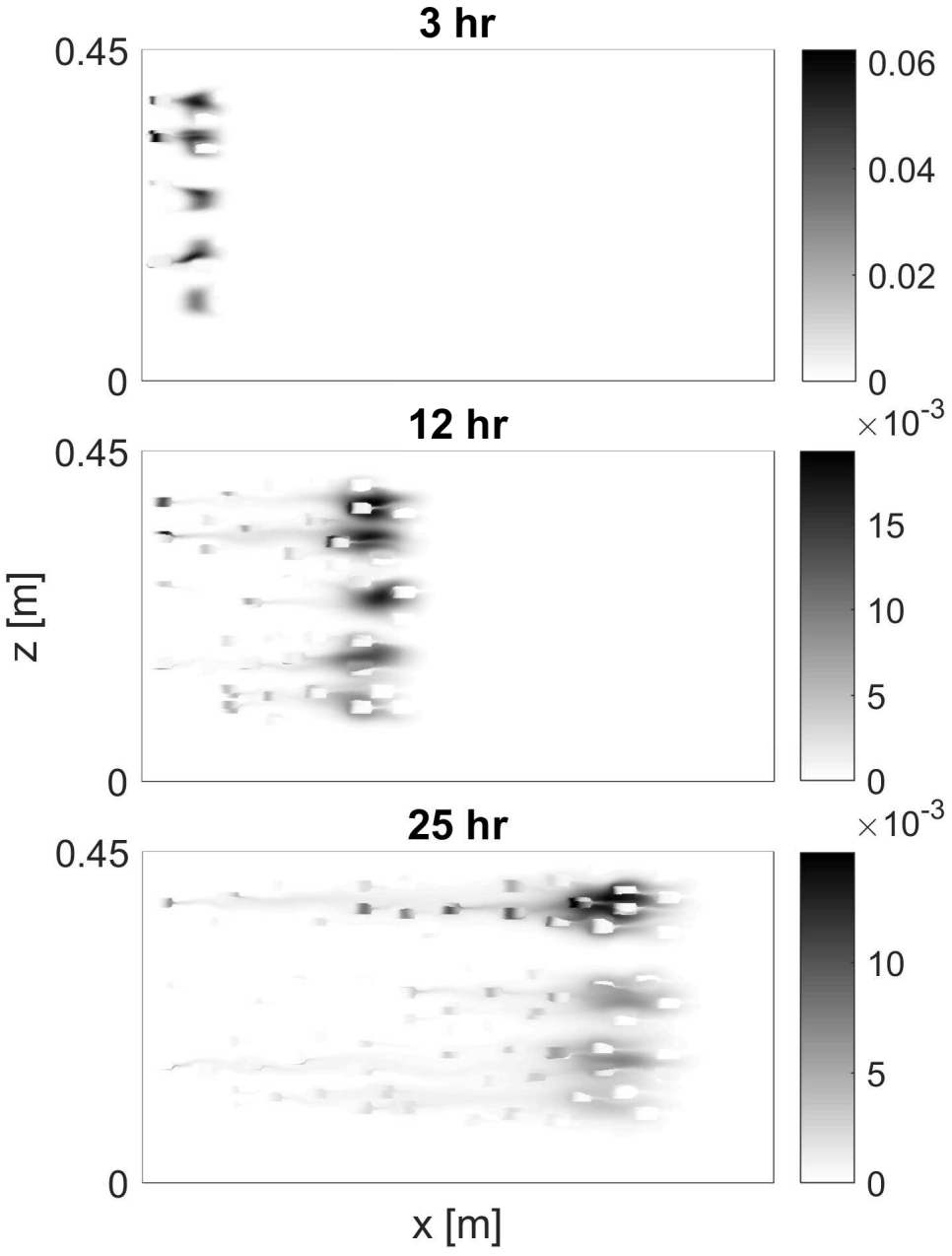

Figure 2: Illustration of numerically simulated conservative solute plumes at 3, 12, 25 hours after initial injection. The hydraulic conductivity field of Case 1 (Figure 1a) was selected for this transport simulation.

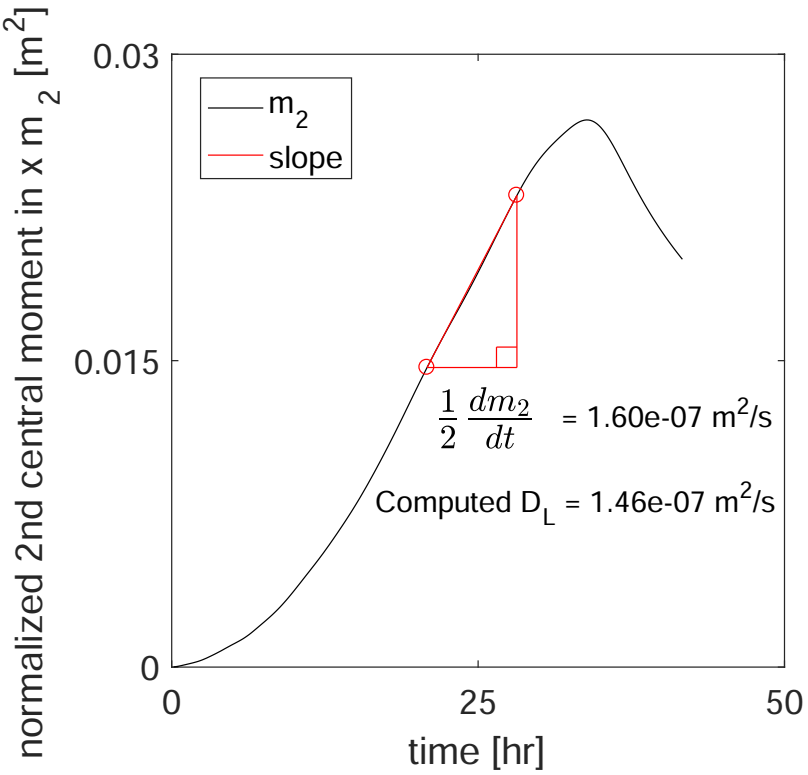

Figure 3: Normalized second central moment vs. time for longitudinal dispersion coefficient computation; the slope was computed from the time it shows a linear behavior to the time when the plume reaches the outlet. The longitudinal dispersion coefficient using the moment analysis with the transient simulation is close to the one computed from the proposed method.

surprisingly small considering that our methodology computes the dispersion coefficient for the whole block while the result from the moments analysis are from mini-plumes that depend on initial conditions, the path they follow, and are limited to be inside the block.

Figure 2 shows the origins of the process of dispersion. At the front of the plume, where the concentration is increasing, there is more mass in the higher-conductivity background sand. In the back, the opposite is true as the concentration is higher in the low-conductivity inclusions and gradually bleeds out into the high-conductivity background. The instantaneous rate of increase of the second moment in the direction of flow depends on the distribution of mass and the velocities where there is mass.

Let us consider the computation of the longitudinal dispersion coefficient. We know that f_1 must satisfy Eq. 11 and that if f_1 satisfies this equation so does f_1' that is obtained after subtracting its mean. By the way it was introduced, C' has zero average over a numerical block Ω, and that is why we want f_i' to be zero on the average. So, our approach is to find any f_1 solution and then subtract the mean. Let us investigate the effect of boundary conditions. In general, f_1' at the boundaries cannot be specified precisely with only grid-scale information. If advection dominates, the effect of the source terms overshadows the effects of the boundary conditions. The fluctuations f_i' are expected to be primarily determined by the fluctuations of velocity when the problem is advection dominated (large Péclet number). Thus, solving with the simplest boundary condition, Dirichlet with constant value, should be adequate for such cases. To test the robustness of this approximation, we systematically investigate the influence of the boundary conditions. We considered all possible combinations of first-type and second-type boundary conditions. The model was run with either zero concentration or no dispersive flux boundary conditions ($D_{local}\frac{\partial f_1}{\partial n} = 0$) imposed on the left, right, top and bottom boundaries separately, resulting in $2^4 - 1 = 15$ combinations. Here, we will present results for Case 1 and Case 4. Boxplots of computed dispersion values with these 15 boundary conditions at different velocities are displayed in Figure 4 showing that only when groundwater is almost stagnant, the boundary conditions affect the computed longitudinal dispersion values. This is expected when we consider a large block for dispersion coefficients in Eq. 15, the covariation term $u'C'$ at the boundaries would not affect the entire dispersion.

Next, we perform additional tests to investigate whether the longitudinal dispersion coefficient as computed by our method depends on the flow direction. Previously tested flow direction is reversed while other parameters are kept same, then the longitudinal dispersion coefficients are computed for Case 1 and Case 4 as shown in Figure 5. The effect of the flow direction is from the assumed boundary condition: For an asymmetric block, the direction of flow has a small effect due to the imposition of zero advective flux on the boundary. The results show that this is small with relative difference no more than 5%, satisfying the condition that the assignment of dispersion coefficient in the numerical model should be independent of the flow direction. We do not mean to underestimate the importance of the role of boundary conditions on computed dispersion; but at least for now we have demonstrated that in the case of longitudinal dispersion and large Péclet number

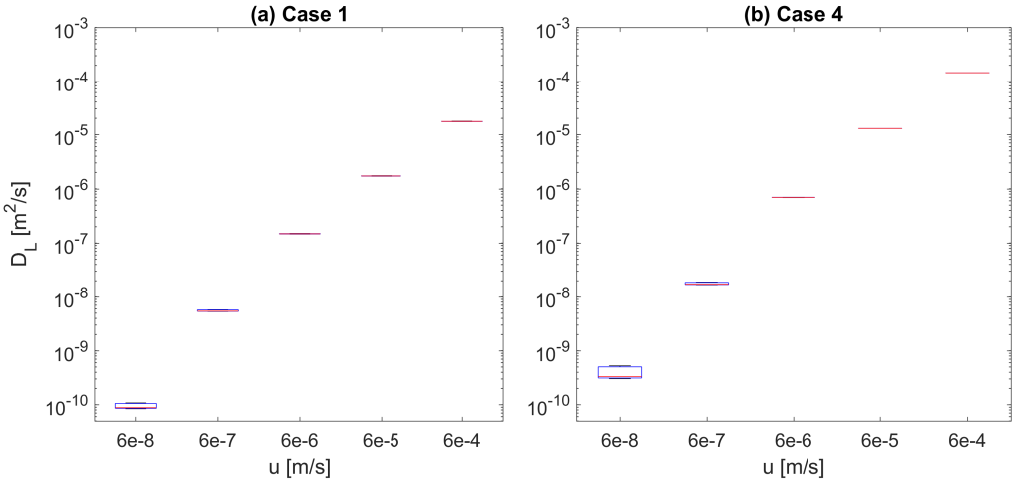

Figure 4: Boxplots of D_L computed with different boundary conditions for Case 1 (a) and Case 4 (b).

the effect of the boundary condition is minor.

We have also compared our method with classical first order analysis based on perturbation theory [32]. Details about such comparison can be found in AppendixA and show an excellent agreement between the values of D_L computed with the two methods for the cases examined (i.e., mildly heterogeneous stationary conductivity fields with small correlation length compared to the size of the block).

Lastly, we investigate what is the relaxation time, which strictly speaking means the time for initial conditions to be forgotten and practically steady state to be achieved as assumed in Eq. 11. But what is an even more important and relevant feature of relaxation time is that changes in ambient conditions with periods much larger than the relaxation time are gradual and the time derivative can be neglected. With the numerical setup investigated earlier (i.e., Case 1 and Case 4 with $\bar{u} = 6 \times 10^{-6}\ m/s$), we perform a transient simulation with initial condition $f = 0$, which is considerably different from the final solution, over the domain and compare transient solutions with the steady-state solution. Figure 6 (a) shows a relative difference between transient and steady-state solutions indicating that at about 70 (Case 1) and 150 (Case 4) hours their relative difference becomes smaller than 1 %. The time to reach the steady state is roughly equal to travel time in the entire domain

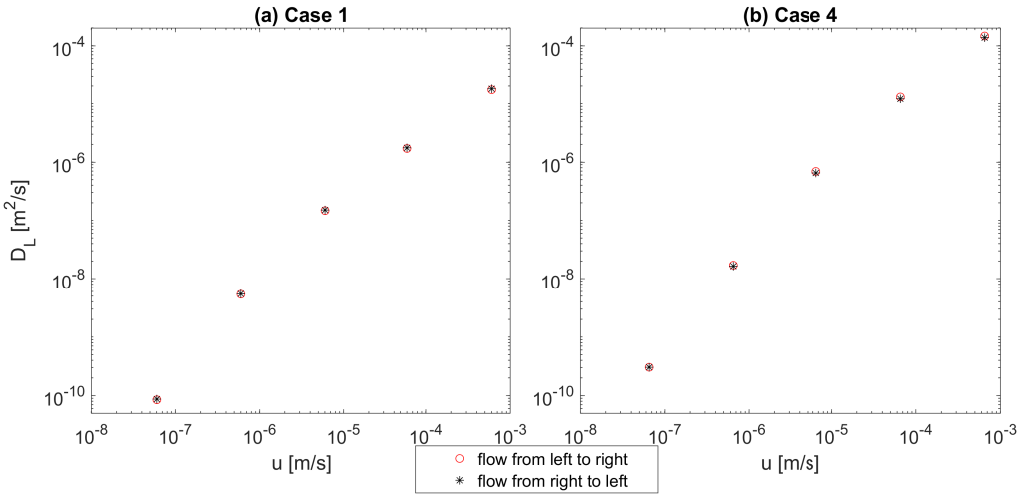

Figure 5: Comparison of D_L with reverse flow condition for Case 1 (a) and for Case 4 (b).

plus diffusion time into the stagnant zones from the matrix. The travel time is $L_x/\bar{u}$ where L_x is the length of the block and $\bar{u}$ is mean velocity; diffusion time is $d^2_{lowK}/D_{local,lowk}$ where d_{lowK} is thickness of inclusion and $D_{local,lowK}$ is local dispersion-diffusion coefficient. More importantly, as shown in Figure 6 (b), the block-effective longitudinal dispersion coefficient becomes practically the same as the one obtained from the steady-state equation after around only 20 and 100 hours for Case 1 and Case 4, respectively. This indicates that the value of the dispersion coefficient is not very sensitive to the assumption that the time derivative can be neglected. This is an important point because changes in most of the domain are bound to be gradual with periods much large than these times. Only near injection points may the conditions change rapidly and thus not conform with the assumption of local equilibrium.

It is important to clarify that local equilibrium does not mean that conditions do not change but only that the conditions change slowly enough. Using a smaller block as a consequence of using a finer grid reduces the relaxation time and thus makes the local equilibrium condition easier to achieve. Also, local equilibrium does not mean that the concentration in low-conductivity zones is the same as the concentration in high-conductivity ones. Rather the opposite is true, since dispersion originates from the fact that mass is distributed between high and low conductivity areas.

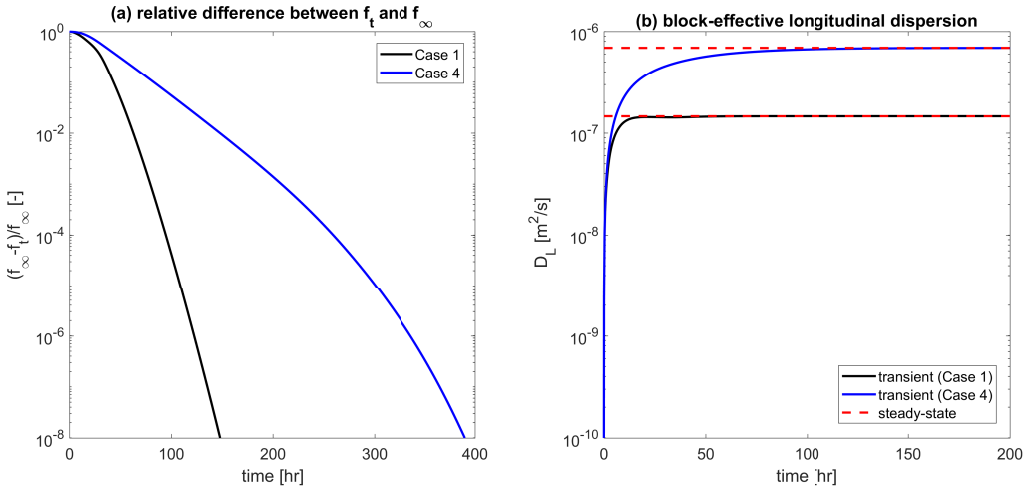

Figure 6: (a) The relative difference between the steady-state solution f_∞ and transient solutions f_t in terms of $|\frac{\int f_\infty dV - \int f_t dV}{\int f_\infty dV}|$ (b) Longitudinal dispersion coefficients for Case 1 and Case 4.

5. Results of Numerical Simulations

In this section, we apply the proposed approach to investigate the block-effective longitudinal dispersion for different geometry of the inclusions, permeability contrast, flow velocity, and local diffusion-dispersion coefficients. For illustration, Figure 7 shows the velocity fluctuation $u_1^{'}$, normalized concentration fluctuation $f_1^{'}$, and their product $u_1^{'} f_1^{'}$ for Case 1 with var(ln K) = 1.69. What determines the magnitude of dispersion is the degree that velocity fluctuations correlate with higher concentrations fluctuations. The fluctuations are similar in appearance to what one sees at the front of a plume, as in Figure 2: Higher values in the high-velocity parts and low velocity in the low permeability inclusions. It is also the negative of what one sees at the back of the plume. That's where the similarity stops, however, because for an individual plume the mean transport velocity at the front is higher than at the back; hence the fast breakthrough and long tail. In our analysis, there is no front and back because only captures a part of a larger plume. One can see that the locations responsible for the generation of dispersion are the low-conductivity inclusions because that is where both velocity and concentration fluctuations are the largest and are the most correlated.

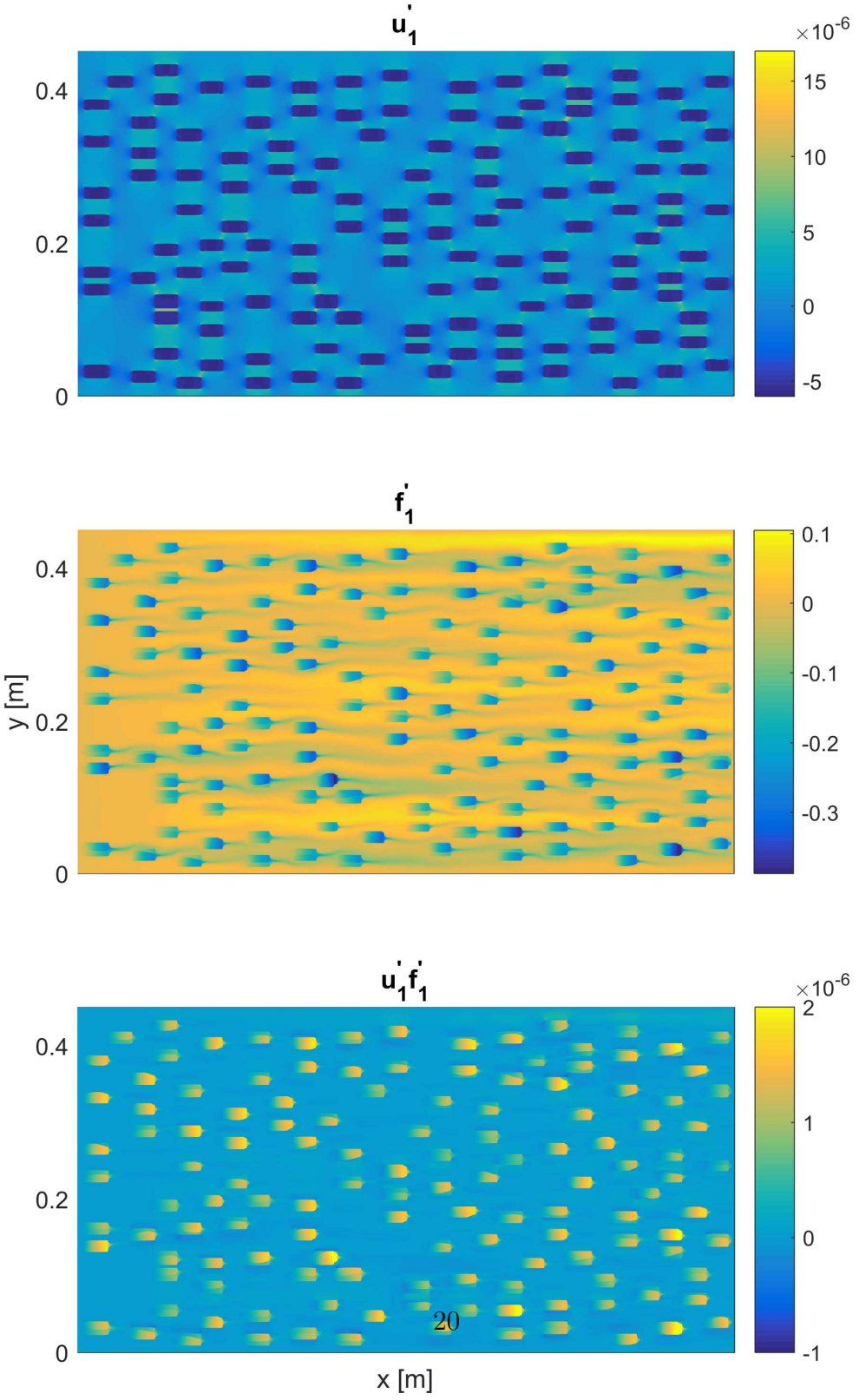

Figure 7: Velocity fluctuation u_1', normalized concentration fluctuation f_1' and the covariation term $u_1' f_1'$ for Case 1 with $\mathrm{var}(\ln K) = 1.69$ and $\bar{u} = 6 \times 10^{-6}$ m/s

The image of normalized concentration fluctuation $f_1^{'}$ reveals the microstructure of velocity fluctuations. One can see that these fluctuations are determined mainly by the fluctuations in velocity and one can see how local dispersion, though it is small, may have some effect because it acts over steep slopes and over the whole domain. One can also see why higher local dispersion coefficients suppress $f_1^{'}$ and thus lower the value of the hydrodynamic dispersion coefficient for the block.

The covariation term $u_1^{'}f_1^{'}$ is plotted for the four cases investigated in Figures 8 and 9, considering mild and high heterogeneity. These maps are illustrative since they allow visualizing where the dispersion originates from, as well as the distinct features and spatial distribution of the covariation term in the domains with different geometry of the low-permeability inclusions. Positive values add to dispersive mixing and negative values subtract. All figures show that the low-permeability inclusions are closely associated with the generation of dispersive fluxes. This of course is because most mass moves with about the same velocity in the permeable background sand whereas the mass in inclusions moves more slowly. The geometry of inclusions plays an important role and higher values of the covariation term are computed for the elongated structures. If there were no local mixing, mass entering inclusions would travel the whole length through advection alone and would be more delayed compared to mass in the permeable background matrix, which would result in higher dispersion rates. At the other extreme, large transverse local dispersion would allow mass to escape from the slow flow zones, reducing dispersion rates. The pictures we see are the result of interplay between advection and diffusive mass transfer in the heterogeneous block at the fine scale (cf. [60]). In fact, in the cases with elongated inclusions (Case 3 and Case 4) mass transfer limitations between the permeable matrix and the low K zones have a significant effect; the less the local mass transfer rates the higher the hydrodynamic dispersion at the block scale. The patterns of $u_1^{'}f_1$ is similar for the mild and high heterogeneity setups but the magnitude is different and, with high contrast structures, more dispersion is generated due to the stronger effect of low velocity and limited mass transfer in the slow zones.

Figure 10 shows the computed block-effective longitudinal dispersion coefficient normalized by molecular diffusion for the four heterogeneous domains (Figure 1), considering a range of grid Péclet numbers ($Pe = \bar{u}l/D_{aq}$, where $l = 0.001$ m is the grid size) including groundwater flow velocities characteristic of most hydrogeologic applications. In each case, three low K values of

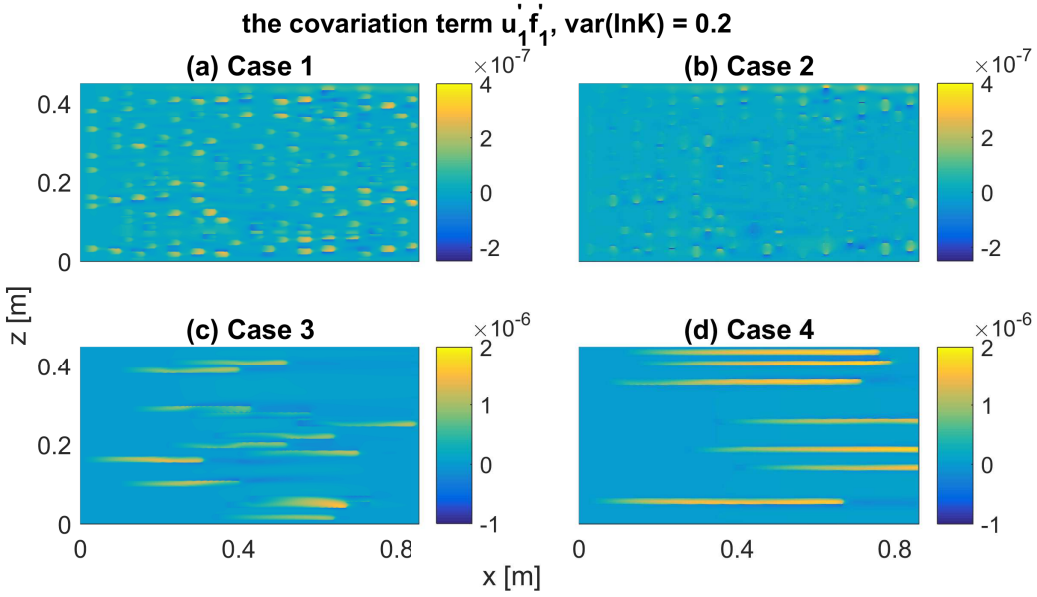

Figure 8: The covariance term $u_1^{'}f_1$ for each case with mildly heterogeneous K (var(ln K) = 0.2) and $\bar{u} = 6 \times 10^{-6}$ m/s.

1.4×10^{-4} (blue), 1.4×10^{-5} (red) and 1.4×10^{-6} (black) m/s were considered to investigate the effect of permeability contrast on the upscaled dispersion coefficients.

For the mildly heterogeneous (var(ln K) $\leq$ 1) K fields with small inclusions (Case 1 and Case 2, blue circles), effective longitudinal dispersion scales linearly with velocity almost throughout the entire range of Péclet numbers ($Pe = 10^{-1}$–10^{3}), showing that the Scheidegger parameterization for the upscaled, effective longitudinal dispersion coefficient is valid in this velocity regime. The results of the numerical experiments can be also clearly visualized by plotting the normalized block-effective dispersivity as D_L/ul as function of Péclet number, which becomes constant for the advective regime ($Pe \geq$ 5 - 10) (Figures 11 (a) and (b)). Note that in the low Péclet number regime ($\sim 10^{-1}$) where the block-effective dispersivity has not yet reached a constant value, molecular diffusion is the main mechanism contributing to dispersion. For the K fields with longitudinally elongated inclusions (Case 3 and Case 4, blue circles), normalized dispersion does not become constant until $Pe = 100$ because of the effect of diffusion and mass transfer limitations. However, in these mildly heterogeneous domains, the Scheidegger

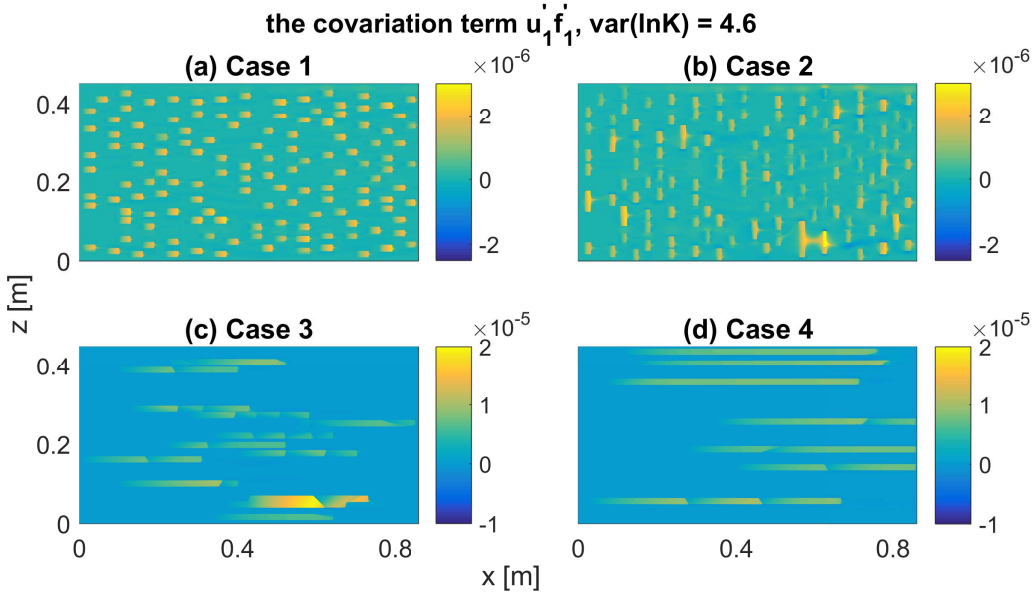

Figure 9: The covariance term $u_1^{'} f_1$ for each case with highly heterogeneous K (var(ln K) = 4.6) and $\bar{u} = 6 \times 10^{-6}$ m/s.

parameterization is likely to work well in practice because the change in actual dispersion coefficient is small thus the assumption may not change significantly the results of transport simulations.

For mid-to-highly heterogeneous (var(ln K) > 1) configurations, red and black markers in Figures 10 and 11, the values of block-scale longitudinal dispersion are considerably higher. The trend of D_L still shows the almost-linear relationship to Pe for the cases with small low-permeability inclusions, (a) and (b). In fact, in these setups the stagnant flow zones are relatively small compared to the entire block length and advection is more important than diffusion, thus suggesting that the Scheidegger parameterization is still valid for these cases. The normalized longitudinal dispersivities in Figures 11 (a) and (b) are shown to be constant for Pe ≥ 50, and for $1 <$ Pe < 50, the transitional or power-law regime [61, 62] is observed where both advection and diffusion affect the effective dispersion. Dispersivity for Case 2 is less variable over the entire range of Pe compared to one for Case 1 because the length of the vertical low-permeability inclusions along the flow direction is shorter so that diffusion affects the dispersion less significantly.

The observed behavior is different for the last two heterogeneous configu-

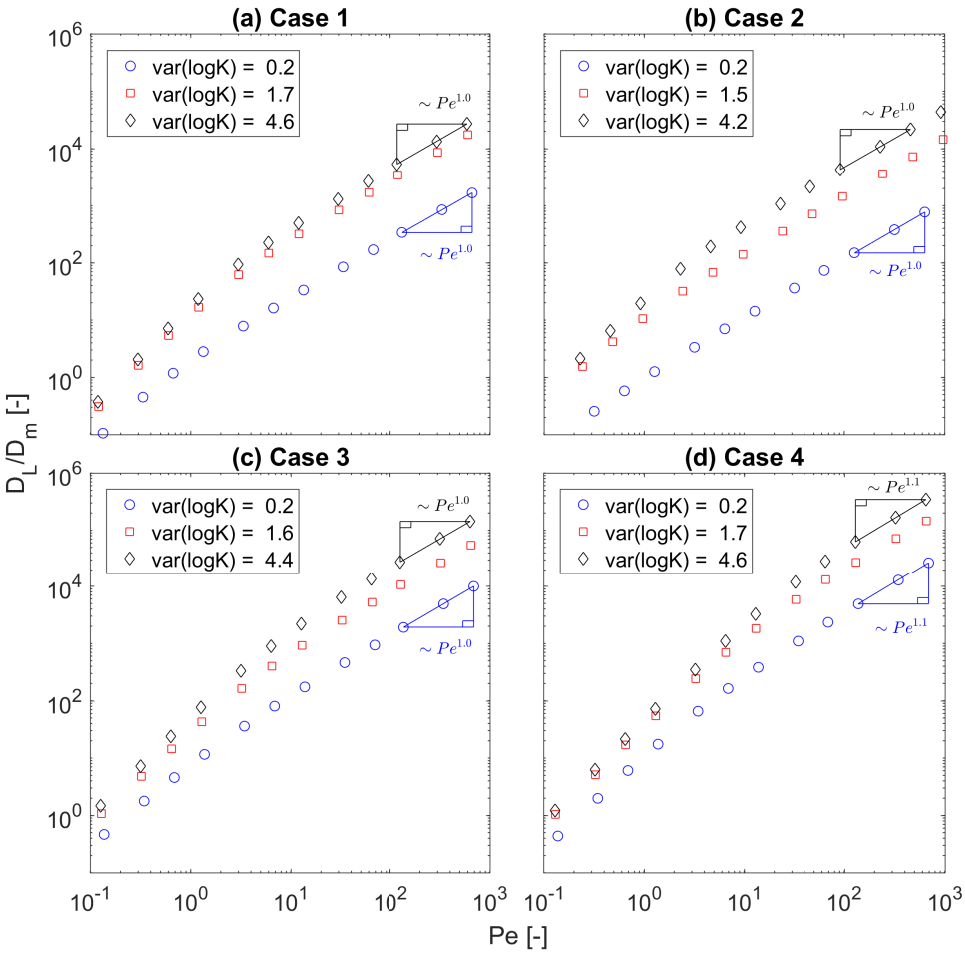

Figure 10: D_L/D_m vs. Pe for four example cases with different heterogeneity.

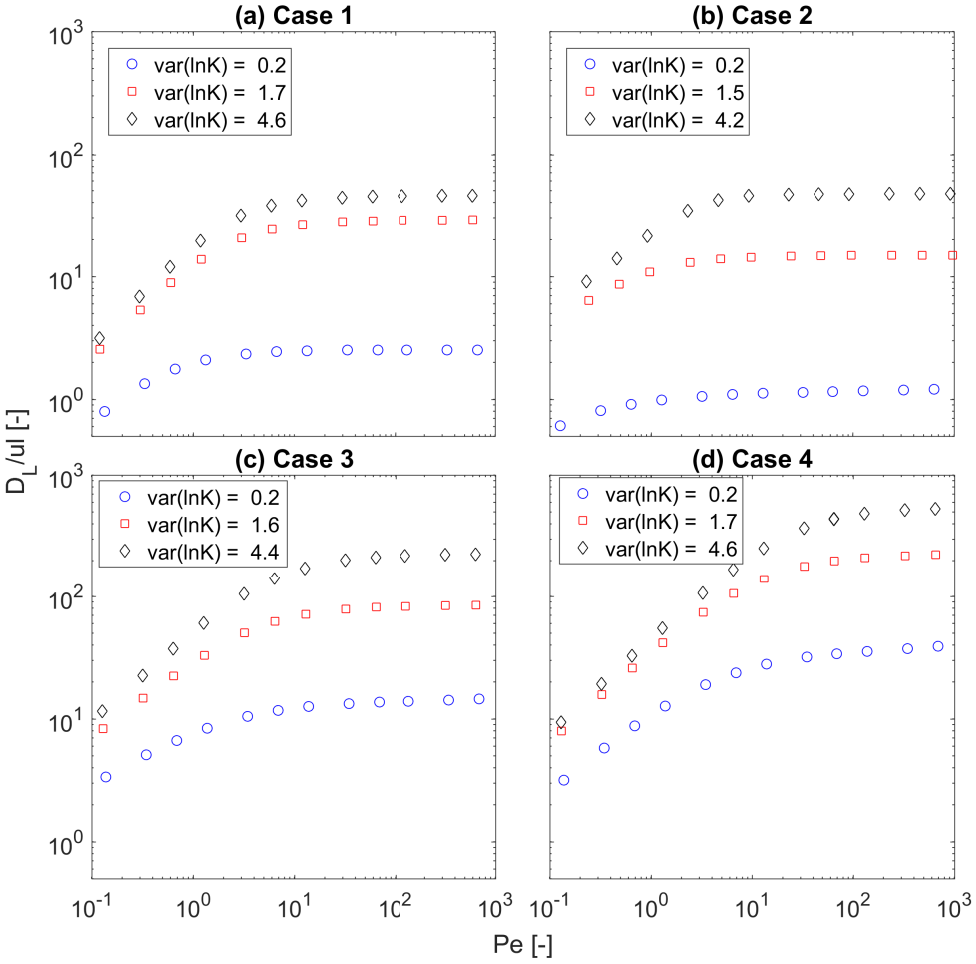

Figure 11: Normalized D_L vs. Pe for four four cases with different heterogeneity.

rations (panels c and d) in Figures 10 and 11. The elongated shape of the low K inclusions and their small permeability results in higher effective longitudinal dispersion and cause a deviation from the linear relationship between the computed D_L and the Péclet number. In these setups high dispersion values originate from mass transfer limitation between the flowing fluid in the high permeable area and immobile pore volume in the low permeable lenses. In fact, the elongated geometry of the inclusions along the main flow direction results in diffusive mass transfer limitation over larger interfaces between the permeable matrix and the low permeable material within the inclusions. Solute in low-permeability zones is forced to move slowly, unless diffusion allows it to escape sideways; thus, diffusion plays an important role in how much dispersion will actually take place. Slow mass transfer causes considerable variability in the velocity and concentration fluctuations, which results in larger dispersion. For these configurations the effective dispersivity can approach a constant values only at very large Péclet numbers. The outcomes of the numerical experiments in the different setups clearly shows that effective dispersion is sensitive to the permeability contrast and to the structure of K.

We have also performed multitracer computational experiments to evaluate the influence of compound-specific aqueous diffusion coefficients on the upscaled effective longitudinal dispersion. We consider a multispecies solute transport problem with four tracers, with different aqueous diffusion coefficients ($D_{aq} = 10^{-10}, 5 \times 10^{-10}, 10^{-9}, 2 \times 10^{-9}\ m^2/s$), simultaneously transported in the heterogeneous domains. Such variability of aqueous diffusion coefficients covers a representative range of aqueous solute diffusivities in groundwater transport problems [63]. The outcomes of the multitracer simulations are reported in Figure 12 as upscaled, block-effective longitudinal dispersivity, α_L, as a function of the seepage velocity for the four configurations of heterogeneous porous media, considering small ($\mathrm{var}(\ln K)$=0.2) and large ($\mathrm{var}(\ln K)$=4.6) conductivity contrasts. The results show different effective dispersivity under diffusion-dominated conditions and very low flow velocity with larger values of α_L for the solutes with lower aqueous diffusion, particularly when a large contrast of hydraulic conductivity between the matrix and the inclusions is considered. Such behavior shows the importance of compound-specific mass-transfer limitations in which solutes with lower aqueous diffusivity undergo a more pronounced longitudinal spreading in the heterogeneous domain. When the flow regime becomes advection-dominated (i.e., higher values of seepage velocity), the outcomes are different for the

distinct cases. With small, distributed inclusions (Case 1 and Case 2) the effective dispersivity converges to a unique value, independent of the diffusion coefficient of the transported species. With elongated low-permeability inclusions (Case 3 and Case 4) the results show a distinct value of effective α_L for the different solutes, particularly when a large contrast of hydraulic conductivity between the matrix and the inclusions is considered. Finally, at very large velocities the effective α_L for the different solutes converges to a constant value as observed for the cases with small inclusions (Figures 12a and 12b).

6. Discussion

Opinions diverge in Hydrogeology regarding the topic of hydrodynamic dispersion in geologic formations. Some apparently do not even consider dispersion as a process of fundamental physical significance, but rather an artifact of how velocity is resolved. However, unless one can resolve velocity variability at the scale of millimeters or less, the effects of unresolved variability are real and indeed prominent. The heterogeneity encountered in geologic formations is both pronounced and highly structured and has major effects on the way solute plumes are conveyed and dispersed. Numerical models are increasingly used to solve flow and transport problems in such heterogeneous formations. This work has dealt with the persistent practical question then is how to capture the effects of velocity variability at scales smaller than those resolved by the grid used in the numerical method. It has re-examined the validity of the Fickian model and the Scheidegger parameterization of dispersion coefficients, which are widely used and yet widely disputed.

Plumes exhibit scale-dependent rates of spreading, irregular shapes, fast breakthrough, and long tails [64, 65], all of which seem to invalidate the Fickian model. However, whether dispersive transport at the scale of a block in a numerical model is Fickian or non-Fickian is a completely different issue [66]. The reason is simply that dispersion of plumes and dispersion in a single block are processes evolving at different scales. It is important to appreciate that the grid should be fine enough to resolve the variability of concentration at the desired level, and thus the grid size should be one tenth or even less than the smallest wavelengths of the concentration variability that must be represented. This is the case for all numerical models, even flow models like MODFLOW [e.g., 67]. Otherwise, there is significant error in representing a function by discrete values, independently of the model and parameters used

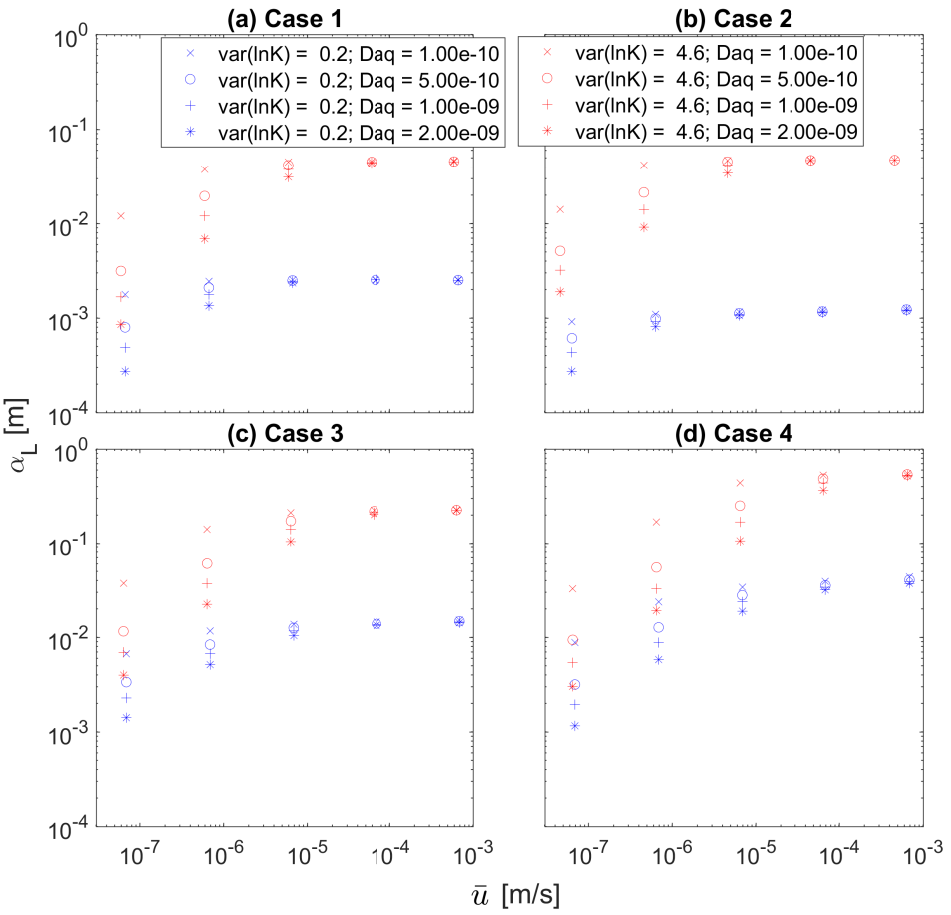

Figure 12: Longitudinal dispersivity α_L vs. $\bar{u}$ for four different tracers with $D_{aq} = 10^{-10}, 5 \times 10^{-10}, 10^{-9}$, and 2×10^{-9} m^2/s.

to solve the flow or transport problem. Associated with this requirement is that changes are not rapid, because rapid changes create spatial fluctuations, like advancing fronts, at scales smaller than those that the model can resolve. These issues are known and are the reason why the grid size must be chosen carefully [68] and variable grid size must often be employed. If a coarse grid is selected important features of heterogeneity but also variability in the concentration may be left out; in any case, one cannot hope that the model can predict at scales not resolved by the model.

The method of analysis in this work defines the problem as how to capture the effects of unresolved small-scale heterogeneity on the resolved grid-scale variability of concentration. We show that under certain conditions these effects are captured by the Fickian model. The conditions are pretty much the same as the requirements that the proper grid has been selected, i.e. gradually varying concentration. In many applications, concentration varies gradually in space and time as plumes transport and evolve over decades. For such problems, the Fickian model for block-dispersion is appropriate. In some other applications, like field experiments or at site remediation near injection points, the concentration function may change rapidly. Thus, the condition of local equilibrium conditions in a block are not met and the Fickian model may be inaccurate. In such a case, one can either select to refine the grid or to adopt a non-equilibrium model like dual domain dual porosity (DDDP). It is important to recognize, though, that the issue is not whether an equilibrium or a non-equilibrium model is right for a certain formation but how fast the changes are in relation to the relaxation time of a block. For example, even if we consider that a medium conforms to the ideal DDDP model but the imposed changes are slow in relation to the characteristic time for the two domains to equilibrate, then effectively the DDDP medium acts as a single domain medium with a certain dispersion coefficient [69, 70, 71].

The next issue we examine is whether the dispersion coefficient is a characteristic of the block and the solute and can be parameterized by using resolved quantities of velocity and concentration. The answer is mostly yes, but there is a small effect from unresolved velocity and concentration fluctuations in neighboring blocks as shown in Figures 4 and 5. The uncertainty from these effects is negligible under ideal conditions, like stationary variability with correlation length small in relation to the size of the block. Even for more unfavorable cases, the uncertainty is small, particularly for large-velocity cases, for which dispersion matters most. In this work, we chose to keep it simple and just quantify the uncertainty rather than seek better

methods to account for the effects from fluctuations in neighboring blocks.

Next, we consider the validity of the standard Scheidegger parameterization, expressed through dispersivity coefficients. We study through computational experiments longitudinal dispersion in a certain direction. The results indicate that the Scheidegger parameterization is a good approximation for stationary media, such as those with multiple small inclusions of low-permeability in a higher-conductivity background as shown by the simulation of Case 1 and Case 2 (panels a and b in Figures 10 and 11). However, geologic heterogeneity is structured, for example clay laminae with preferential orientation are much more likely than clay lumps randomly distributed. For such cases (e.g., Case 3 and Case 4), the Scheidegger limit is reached only for large Pe (see panels c and d in Figures 10 and 11). For velocity values in the commonly encountered range, the effective dispersivity gradually increases over two orders of magnitude and at high velocity values can have a much larger value than the ones used in practice, equaling or even potentially exceeding the dimension of the block. Interestingly, two different solutes, with distinct molecular diffusion coefficients, experience different rates of hydrodynamic dispersion and in fact the one with lower molecular diffusion coefficient experiencing a higher dispersion rate as shown in Fig 12. These are features that are usually not included in modeling studies.

The analysis carried out in this work allowed us to investigate block-scale longitudinal dispersion in heterogeneous domains with different permeability contrast and geometry of low-permeability inclusions. Particular attention has been dedicated to explain and visualize the origin of block dispersion from velocity and concentration fluctuations, to analyze the interplay between the fundamental processes of advection and diffusion, and to investigate the important role of mass transfer limitations in determining the values of effective dispersion. The method is rigorous but, at the same time, simple enough to be appealing for both researchers and practitioners interested in modeling groundwater transport problems. As we discussed above, the method is not unconditionally valid since it is subject to the requirements of gradual changes leading to a condition of physical equilibrium. However, as we have shown in our analysis these conditions are not particularly restrictive and apply to many situations typically encountered for transport of contaminant plumes in the subsurface. Therefore, we believe that the proposed approach can represent a significant step forward to improve our capability to accurately describe solute transport in heterogeneous formations. We also hope that the method could contribute to shorten the distance between academia

and practice in a field of Hydrogeology that is inherently complex and rich of future challenges in terms of process understanding, methods' development, and practical engineering applications.

7. Acknowledgment

JL and PKK acknowledge the support of the National Science Foundation through its ReNUWIt Engineering Research Center (www.renuwit.org; NSF EEC-1028968) and the Army High Performance Computing Research Center (AHPCRC, sponsored by the U.S. Army Research Laboratory under contract No. W911NF-07-2-0027) at Stanford University. JL was supported in part by an appointment to the Postgraduate Research Participation Program at the U.S. Army Engineer Research and Development Center, Coastal and Hydraulics Laboratory (ERDC-CHL) administered by the Oak Ridge Institute for Science and Education through an interagency agreement between the U.S. Department of Energy and ERDC. The compute resources for this project were provided under the AWS Cloud Credits for Research Program. The authors would like to thank Olaf Cirpka for providing an earlier version of the numerical code that was used in this study.

AppendixA. Stationary Conductivity

This section summarizes results of numerical experiments for the case of stationary conductivity with correlation length that is small compared to the size of the block. For small variance, the classical first order analysis based on perturbation theory [e.g., 32, 17] predicts that the whole-domain or large-block dispersivity in the longitudinal direction is

$$\alpha_L = \sigma^2_{\ln K} I_{\ln K,x} \tag{A.1}$$

where $\sigma^2_{\ln K}$ is the variance of the log-K field and $I_{\ln K,x}$ is the integral scale in the x direction, which concurs with the length parameter for the isotropic exponential covariance function. We will use it to compute the block coefficient and compare with our results.

First, we consider the longitudinal dispersivity using the small-perturbation method for 2-D log-normal random fields whose geometric mean is $10^{-3}\ m/s$ and covariance function is exponential, $\sigma^2_{\ln K}\exp(-\frac{r}{L})$, where r is the distance between two spatial points, with scale parameter $L = 0.01\ m$ and $\sigma^2_{\ln K} = 0.1,\ 0.25$ and 0.5. From theory, their whole-domain dispersivity

$\sigma^2_{\ln K}$	dispersivity α_L [m]	
	perturbation theory	proposed method
0.1	1.0×10^{-3}	1.01×10^{-3}
0.25	2.5×10^{-3}	2.60×10^{-3}
0.5	5.0×10^{-3}	5.09×10^{-3}

Table A.2: Comparison of dispersivity α_L from the small-perturbation theory and using the proposed method; mean block-effective dispersivity was computed from 100 realizations from multidimensional log-normal distribution with an exponential covariance kernel $\sigma^2_{\ln K} \exp(-\frac{r}{L})$ where r is the distance between two spatial points, $L = 0.01$ m and $\sigma^2_{\ln K} = 0.1$, 0.25 and 0.5.

is $L \times \sigma^2_{\ln K} = 0.001$, 0.025 and 0.005, respectively due to the equivalence between the integral scale and the scale parameter L for the exponential covariance kernel. Then, we generate 100 realizations for each log-random K field and compute the block-effective dispersivity $\alpha_L = D_L/\bar{u}$. The size of the domain we consider here is 1 $m \times 1$ m and discretized with $dx = dy = 0.001$ m. A realization of $\ln K$ field is shown in Figure A.13 (a). Constant head boundaries of 0.05 and 0 m are imposed at $x = 0$ and 1 m, respectively with no-flux at $y = 0$ and 1 m that creates mean flow velocity in x-direction of around 1.0×10^{-4} m/s for each realization corresponding to $Pe = 100$. Local dispersion parameterizations used in this study are same as those used in the previous numerical experiments, i.e., Eqs. 16 and 17 with $D_{aq} = 10^{-9}$ m^2/s.

In Table A.2, the block-effective dispersivity values are computed from 100 realizations for three different variance cases and compared with dispersivity obtained from the perturbation method. The results show that the proposed method yields consistent dispersivity values to the one obtained from the perturbation method.

[1] R. C. Acharya, A. J. Valocchi, C. J. Werth, T. W. Willingham, Pore-scale simulation of dispersion and reaction along a transverse mixing zone in two-dimensional porous media, Water Resources Research 43 (2007).

[2] A. M. Tartakovsky, G. D. Tartakovsky, T. D. Scheibe, Effects of incomplete mixing on multicomponent reactive transport, Advances in Water Resources 32 (2009) 1674–1679.

[3] H. Yoon, A. J. Valocchi, C. J. Werth, T. Dewers, Pore-scale simulation

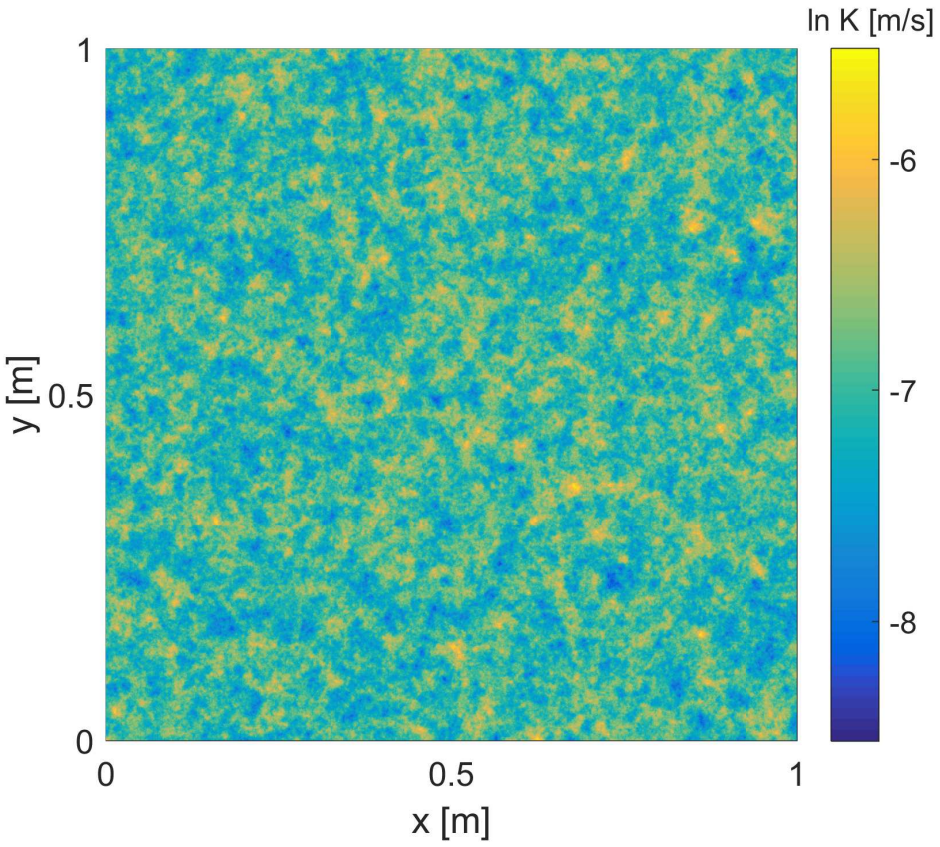

Figure A.13: A realization of $\ln K$ field with $\sigma^2_{\ln K} = 0.1$.

of mixing-induced calcium carbonate precipitation and dissolution in a microfluidic pore network, Water Resources Research 48 (2012).

[4] M. Icardi, G. Boccardo, D. L. Marchisio, T. Tosco, R. Sethi, Pore-scale simulation of fluid flow and solute dispersion in three-dimensional porous media, Physical Review E 90 (2014).

[5] M. Rolle, P. K. Kitanidis, Effects of compound-specific dilution on transient transport and solute breakthrough: A pore-scale analysis, Advances in Water Resources 71 (2014) 186–199.

[6] D. W. Meyer, B. Bijeljic, Pore-scale dispersion: Bridging the gap between microscopic pore structure and the emerging macroscopic transport behavior, Physical Review E 94 (2016).

[7] S. P. Neuman, Universal scaling of hydraulic conductivities and dispersivities in geologic media, Water Resources Research 26 (1990) 1749–1758.

[8] S. E. Silliman, E. S. Simpson, Laboratory evidence of the scale effect in dispersion of solutes in porous-media, Water Resources Research 23 (1987) 1667–1673.

[9] S. P. Neuman, Y. K. Zhang, A quasi-linear theory of non-fickian and fickian subsurface dispersion .1. theoretical-analysis with application to isotropic media, Water Resources Research 26 (1990) 887–902.

[10] E. E. Adams, L. W. Gelhar, Field-study of dispersion in a heterogeneous aquifer .2. spatial moments analysis, Water Resources Research 28 (1992) 3293–3307.

[11] M. Levy, B. Berkowitz, Measurement and analysis of non-fickian dispersion in heterogeneous porous media, Journal of Contaminant Hydrology 64 (2003) 203–226.

[12] M. Moroni, N. Kleinfelter, J. H. Cushman, Analysis of dispersion in porous media via matched-index particle tracking velocimetry experiments, Advances in Water Resources 30 (2007) 1–15.

[13] A. E. Scheidegger, Statistical hydrodynamics in porous media, Journal of Applied Physics 25 (1954) 994–1001.

[14] L. W. Gelhar, Stochastic subsurface hydrology, Prentice-Hall, Englewood Cliffs, N.J., 1993.

[15] G. Dagan, Flow and transport in porous formations, Springer-Verlag, Berlin ; New York, 1989.

[16] Y. Rubin, Applied stochastic hydrogeology, Oxford University Press, Oxford ; New York, 2003.

[17] G. Dagan, Upscaling of dispersion coefficients in transport through heterogeneous formations, Computational Methods in Water Resources X 1 (1994) 431–439.

[18] Y. Rubin, A. Sun, R. Maxwell, A. Bellin, The concept of block-effective macrodispersivity and a unified approach for grid-scale- and plume-scale-dependent transport, Journal of Fluid Mechanics 395 (1999) 161–180.

[19] J. Wang, P. K. Kitanidis, Analysis of macrodispersion through volume averaging: comparison with stochastic theory, Stochastic Environmental Research and Risk Assessment 13 (1999) 66–84.

[20] Y. Rubin, A. Bellin, A. E. Lawrence, On the use of block-effective macrodispersion for numerical simulations of transport in heterogeneous formations, Water Resources Research 39 (2003).

[21] M. Dentz, F. P. J. de Barros, Dispersion variance for transport in heterogeneous porous media, Water Resources Research 49 (2013) 3443–3461.

[22] F. P. J. de Barros, M. Dentz, Pictures of blockscale transport: Effective versus ensemble dispersion and its uncertainty, Advances in Water Resources 91 (2016) 11–22.

[23] D. M., B. T. L., E. A., B. B., Mixing, spreading and reaction in heterogeneous media: A brief review, Journal of Contaminant Hydrology 120 (2011) 1 – 17.

[24] S. P. Neuman, D. M. Tartakovsky, Perspective on theories of non-fickian transport in heterogeneous media, Advances in Water Resources 32 (2009) 670 – 680.

[25] M. Dogan, R. L. Van Dam, G. Liu, M. M. Meerschaert, J. J. Butler, G. C. Bohling, D. A. Benson, D. W. Hyndman, Predicting flow and transport in highly heterogeneous alluvial aquifers, Geophysical Research Letters 41 (2014) 7560–7565.

[26] D. L. Hochstetler, W. Barrash, C. Leven, M. Cardiff, F. Chidichimo, P. K. Kitanidis, Hydraulic tomography: Continuity and discontinuity of high-k and low-k zones, Groundwater 54 (2016) 171–185.

[27] J. Lee, H. Yoon, P. K. Kitanidis, C. J. Werth, A. J. Valocchi, Scalable subsurface inverse modeling of huge data sets with an application to tracer concentration breakthrough data from magnetic resonance imaging, Water Resources Research 52 (2016) 5213–5231.

[28] T. D. Scheibe, C. R. Cole, Non-gaussian particle tracking - application to scaling of transport processes in heterogeneous porous-media, Water Resources Research 30 (1994) 2027–2039.

[29] D. Fernàndez-Garcia, J. J. Gómez-Hernández, Impact of upscaling on solute transport: Traveltimes, scale dependence of dispersivity, and propagation of uncertainty, Water Resources Research 43 (2007).

[30] B. Bijeljic, P. Mostaghimi, M. J. Blunt, Insights into non- fickian solute transport in carbonates, Water Resources Research 49 (2013) 2714–2728.

[31] G. I. Taylor, Diffusion by continuous movements, Proceedings of the London Mathematical Society 20 (1922) 196–212.

[32] G. Dagan, Solute transport in heterogeneous porous formations, Journal of Fluid Mechanics 145 (1984) 151–177.

[33] A. Bensoussan, J. L. Lions, G. Papanicolaou, Asymptotic analysis for periodic structures, Studies in mathematics and its applications, North-Holland Pub. Co. ; sole distributors for the U.S.A. and Canada, Elsevier North-Holland, Amsterdam ; New York New York, 1978.

[34] H. Brenner, A general theory of taylor dispersion phenomena, Physico-Chemical Hydrodynamics 1 (1980) 91–123.

[35] A. Bourgeat, M. Quintard, S. Whitaker, Comparison between homogenization theory and volume averaging method with closure problem, Comptes Rendus De L Academie Des Sciences Serie Ii 306 (1988) 463–466.

[36] O. A. Plumb, S. Whitaker, Dispersion in heterogeneous porous-media .1. local volume averaging and large-scale averaging, Water Resources Research 24 (1988) 913–926.

[37] P. K. Kitanidis, Analysis of macrodispersion through volume-averaging - moment equations, Stochastic Hydrology and Hydraulics 6 (1992) 5–25.

[38] L. W. Gelhar, C. L. Axness, Stochastic-analysis of macrodispersion in 3-dimensionally heterogeneous aquifers, Abstracts of Papers of the American Chemical Society 183 (1982) 74–Inde.

[39] P. K. Kitanidis, Teaching and communicating dispersion in hydrogeology, with emphasis on on the applicability of the fickian model, Advances in Water Resources (2017).

[40] B. Bijeljic, A. Raeini, P. Mostaghimi, M. J. Blunt, Predictions of non-fickian solute transport in different classes of porous media using direct simulation on pore-scale images, Phys. Rev. E 87 (2013) 013011.

[41] V. Kapoor, L. W. Gelhar, Transport in three-dimensionally heterogeneous aquifers: 1. dynamics of concentration fluctuations, Water Resources Research 30 (1994) 1775–1788.

[42] V. Kapoor, P. K. Kitanidis, Advection-diffusion in spatially random flows: Formulation of concentration covariance, Stochastic Hydrology and Hydraulics 11 (1997) 397–422.

[43] R. D. Beckie, Analysis of scale effects in large-scale solute transport models, Cambridge University Press Cambridge, UK, pp. 314–334.

[44] H. P. Amaral Souto, C. Moyne, Dispersion in two-dimensional periodic porous media. part i. hydrodynamics, Physics of Fluids 9 (1997) 2243–2252.

[45] S. E. Silliman, S. Caswell, Observations of measured hydraulic conductivity in two artificial, confined aquifers with boundaries, Water Resources Research 34 (1998) 2203–2213.

[46] J. M. P. Q. Delgado, A critical review of dispersion in packed beds, Heat and Mass Transfer 42 (2006) 279–310.

[47] G. Chiogna, C. Eberhardt, P. Grathwohl, O. A. Cirpka, M. Rolle, Evidence of compound-dependent hydrodynamic and mechanical transverse dispersion by multitracer laboratory experiments, Environmental Science & Technology 44 (2010) 688–693.

[48] J. M. P. Q. Delgado, Longitudinal and transverse dispersion in porous media, Chemical Engineering Research & Design 85 (2007) 1245–1252.

[49] M. Muniruzzaman, M. Rolle, Experimental investigation of the impact of compound-specific dispersion and electrostatic interactions on transient transport and solute breakthrough, Water Resources Research (2017) n/a–n/a.

[50] C. M. Haberer, M. Rolle, S. H. Liu, O. A. Cirpka, P. Grathwohl, A high-resolution non-invasive approach to quantify oxygen transport across the capillary fringe and within the underlying groundwater, Journal of Contaminant Hydrology 122 (2011) 26–39.

[51] M. Rolle, M. Muniruzzaman, C. M. Haberer, P. Grathwohl, Coulombic effects in advection-dominated transport of electrolytes in porous media: Multicomponent ionic dispersion, Geochimica Et Cosmochimica Acta 120 (2013) 195–205.

[52] Y. Ye, G. Chiogna, O. Cirpka, P. Grathwohl, M. Rolle, Experimental investigation of compound-specific dilution of solute plumes in saturated porous media: 2-d vs. 3-d flow-through systems, Journal of Contaminant Hydrology 172 (2015) 33–47.

[53] M. Rolle, D. Hochstetler, G. Chiogna, P. K. Kitanidis, P. Grathwohl, Experimental investigation and pore-scale modeling interpretation of compound-specific transverse dispersion in porous media, Transport in Porous Media 93 (2012) 347–362.

[54] D. L. Hochstetler, M. Rolle, G. Chiogna, C. M. Haberer, P. Grathwohl, P. K. Kitanidis, Effects of compound-specific transverse mixing on steady-state reactive plumes: Insights from pore-scale simulations and darcy-scale experiments, Advances in Water Resources 54 (2013) 1–10.

[55] A. Hazen, Some physical properties of sands and gravels, with special reference to their use in filtration, 24th annual report to the Massachusetts State Board of Health 539 (1892) 539–556.

[56] O. A. Cirpka, F. P. J. de Barros, G. Chiogna, M. Rolle, W. Nowak, Stochastic flux-related analysis of transverse mixing in two-dimensional heterogeneous porous media, Water Resources Research 47 (2011).

[57] D. Eckert, M. Rolle, O. A. Cirpka, Numerical simulation of isotope fractionation in steady-state bioreactive transport controlled by transverse mixing, Journal of Contaminant Hydrology 140 (2012) 95–106.

[58] O. A. Cirpka, E. O. Frind, R. Helmig, Streamline-oriented grid generation for transport modelling in two-dimensional domains including wells, Advances in Water Resources 22 (1999) 697–710.

[59] R. Aris, On the dispersion of a solute in a fluid flowing through a tube, Proceedings of the Royal Society of London Series a-Mathematical and Physical Sciences 235 (1956) 67–77.

[60] A. J. Guswa, D. L. Freyberg, Slow advection and diffusion through low permeability inclusions, Journal of Contaminant Hydrology 46 (2000) 205–232.

[61] J. J. Fried, M. A. Combarnous, Dispersion in Porous Media, volume Volume 7, Elsevier, pp. 169–282.

[62] B. Bijeljic, A. H. Muggeridge, M. J. Blunt, Pore-scale modeling of longitudinal dispersion, Water Resources Research 40 (2004).

[63] M. Rolle, G. Chiogna, D. L. Hochstetler, P. K. Kitanidis, On the importance of diffusion and compound-specific mixing for groundwater transport: An investigation from pore to field scale, Journal of Contaminant Hydrology 153 (2013) 51–68.

[64] L. W. Gelhar, C. Welty, K. R. Rehfeldt, A critical-review of data on field-scale dispersion in aquifers, Water Resources Research 28 (1992) 1955–1974.

[65] J. Carrera, An overview of uncertainties in modeling groundwater solute transport, Journal of Contaminant Hydrology 13 (1993) 23–48.

[66] A. Fiori, G. Dagan, I. Jankovic, A. Zarlenga, The plume spreading in the made transport experiment: Could it be predicted by stochastic models?, Water Resources Research 49 (2013) 2497–2507.

[67] A. M. W. Lal, Numerical errors in groundwater and overland flow models, Water Resources Research 36 (2000) 1237–1247.

[68] T. E. Reilly, A. W. Harbaugh, Guidelines for evaluating ground-water flow models, US Department of the Interior, US Geological Survey, 2004.

[69] Y. Liu, P. K. Kitanidis, Applicability of the dual-domain model to nonaggregated porous media, Groundwater 50 (2012) 927–934.

[70] J. C. Parker, M. T. van Genuchten, Flux-averaged and volume-averaged concentrations in continuum approaches to solute transport, Water Resources Research 20 (1984) 866–872.

[71] J. C. Parker, A. J. Valocchi, Constraints on the validity of equilibrium and first-order kinetic transport models in structured soils, Water Resources Research 22 (1986) 399–407.

Highlights

- Method to compute block-scale effective dispersion based on the Fickian model
- The origin of dispersion within heterogeneous blocks is explained and visualized
- Error quantification for the proposed method and comparison with other approaches
- Validity of classical Scheidegger parameterization for block dispersion is analyzed
- Key role of mass transfer limitations for dispersion in heterogeneous blocks